NuMu Note #187

Emittance Exchange using the Helical Sweeping Method

R.C. Fernow & J.C. Gallardo
Brookhaven National Laboratory

2 January 2001

Abstract

We examine the use of Derbenev's helical sweeping method to reduce the energy spread of a muon beam. We briefly review the basic theory behind the sweeping method and describe the modeling of the magnetic fields in ICOOL. We discuss the efficiency of the method for producing dispersion and for removing energy spread in the beam. We consider the deleterious effects of stochastic processes and finite transverse emittance. Unfortunately, we find that this method is not useful for reducing the energy spread of the beam produced from the neutrino factory target.

1 Introduction

Direct cooling of the longitudinal phase space of a muon beam is very inefficient, so reduction of longitudinal phase space relies instead on emittance exchange [1]. In this process wedge-shaped absorbers in dispersive regions of the magnetic lattice reduce the momentum spread in the beam, while allowing the transverse area of the beam to increase [2]. This represents an exchange of transverse for longitudinal emittance. Derbenev [3] has proposed what he calls the "sweeping method" to reduce the large energy spread of an initially unbunched muon beam. The natural place to apply this idea in the context of the neutrino factory is in the pion decay region immediately following the production target. If the system were very effective at reducing the energy spread, it could eliminate the need for all or part of the following phase rotation system.

The basic idea is to employ a rotating dipole field to generate dispersion in a straight beam channel. A set of wedge shaped absorbers is used in the dispersive region to reduce the energy spread of the beam. A solenoidal field is used to confine the beam. The solenoidal field strength is tapered downwards to match the energy loss of the beam in the absorbers. No *rf* is used to

restore the energy loss, so this method can only be applied over a limited length.

2 Sweeping method

The complete theory of the sweeping method can be found in Derbenev's papers [3]. We review here several of his results of direct importance to these simulations. The dispersion is given by

$$D \approx \frac{k\,a}{k_c - k} \tag{1}$$

where a is the radius of the helical orbit and

$$k_c = \frac{2\pi}{\Lambda_c} = \frac{e\,B}{p}$$
$$k = \frac{2\pi}{\Lambda_w} \tag{2}$$

are the cyclotron and wiggler wave numbers. B is the solenoidal field, p is the particle momentum and e is the particle charge. The sweeping method requires the wiggler wavelength be longer than the cyclotron (or Larmor) wavelength and thus the dispersion will be positive. The radius of the helical orbit is given by

$$a \approx \frac{b}{k\left(B - \frac{k\,p}{e}\right)} \tag{3}$$

where b is the dipole field strength. For B = 6 T, b = 0.2 T, p = 0.5 GeV/c and Λ_W = 2.5 m, we find that a = 4.3 cm and D ~ 9 cm.

3 Modeling of the B field

The magnetic fields used in this simulation consisted of the tapered solenoid and the rotating dipole field. The solenoid B_Z field had a slowly varying linear taper and a corresponding radial component given by

$$B_R = -\frac{1}{2}\frac{dB_Z}{dz}\,r \tag{4}$$

The helical dipole field was given by [4]

$$
\begin{aligned}
B_r &= -C \frac{\left(K_o(ka) + \dfrac{K_1(ka)}{ka} \right)}{\left(I_o(ka) - \dfrac{I_1(ka)}{ka} \right)} \left(I_o(kr) + I_2(kr) \right) \sin(Z) \\
B_z &= 2\,C \frac{\left(I_o(ka) - \dfrac{I_1(ka)}{ka} \right)}{\left(K_o(ka) + \dfrac{K_1(ka)}{ka} \right)} \frac{K_1(ka)}{I_1(ka)} I_1(kr) \cos(Z) \\
B_\varphi &= -\frac{B_z}{kr}
\end{aligned}
\qquad \textbf{(5)}
$$

where

$$
\begin{aligned}
C &= \frac{-2\,\mu_o I k}{\pi} \left[ka\, K_o(ka) + K_1(ka) \right] \\
Z &= \varphi - \varphi_o - kz \\
k &= \frac{2\pi}{\Lambda_w}
\end{aligned}
\qquad \textbf{(6)}
$$

and {a, I, Λ_w, φ_o} are the {radius, current, period, initial orientation} of the helical winding. K_n and I_n are Bessel functions.

ICOOL uses a reference particle based coordinate system. The equations of motion are derived using the Frenet equations [5], which use curvature parameters in both transverse planes and a torsion parameter. ICOOL uses the two transverse curvature parameters, but not the torsion, similar to the treatment by Weidemann [6]. In a helical field the reference particle undergoes a helical trajectory and the tracking gives the coordinates of other particles with respect to this helical orbit. In general these coordinates are not very illuminating and one would prefer to use laboratory coordinates in this situation. A method has been provided to achieve this[1] and all quantities in this report in the helical field are given in laboratory coordinates.

[1] A separate reference momentum is associated with the helical field. If it is set to a very large value, the computed curvature parameters will be very small and the results will correspond to a straight reference trajectory.

4 Generation of dispersion

We first examine how well this helical system generates dispersion. We take an initial, on-axis muon beam with a gaussian distribution of momentum 500±50 MeV/c, 0 bunch length and 0 finite emittance. We use a constant solenoidal field and no wedges in a 40 m long channel. The helical dipole field has a period 2.5 m, dipole strength 0.2 T and a radius 35 cm. The initial orientation of the dipole field is along the *x* axis. We determine the dispersion in the simulation using the linear correlation coefficient *r*, i.e.

$$D_y = r_y \sigma_y = \frac{\langle y p_z \rangle}{\sigma_{p_z}} \qquad \textbf{(7)}$$

and similarly for D_x. Results for the dispersion are shown in Fig. 1. The bottom figure shows the dispersion in a 6 T solenoid field. First of all we see that the helical system does produce dispersion. It varies in azimuthal angle as the beam proceeds down the channel and reaches a peak value around 10 cm, agreeing with the estimate is section 2.

The middle part of Fig. 1 shows that the behavior is similar for a 5 T solenoid field, but the azimuthal variation is changed slightly. Part of the reason for the rotation of the dispersion direction is the different time of flight of particles with different momenta in the solenoidal field. To check this we imposed a transverse momentum on each incident particle that was correlated with its longitudinal momentum.

$$p_\perp = \frac{\sqrt{p_z^2 (1 - \beta_o^2) - m^2 \beta_o^2}}{\beta_o} \qquad \textbf{(8)}$$

where β_o is the desired velocity factor for all the particles. This correlation exactly compensates the longitudinal momentum variation in a pure solenoid, but the correlation is broken by the presence of the weak dipole field. The top part of Fig. 1 shows that the magnitude of the dispersion is larger and is directed along y with less azimuthal variation. We make no further use of this correlation in this report, since there is no way to impose it for the application considered here, namely capture of the pions produced at the production target.

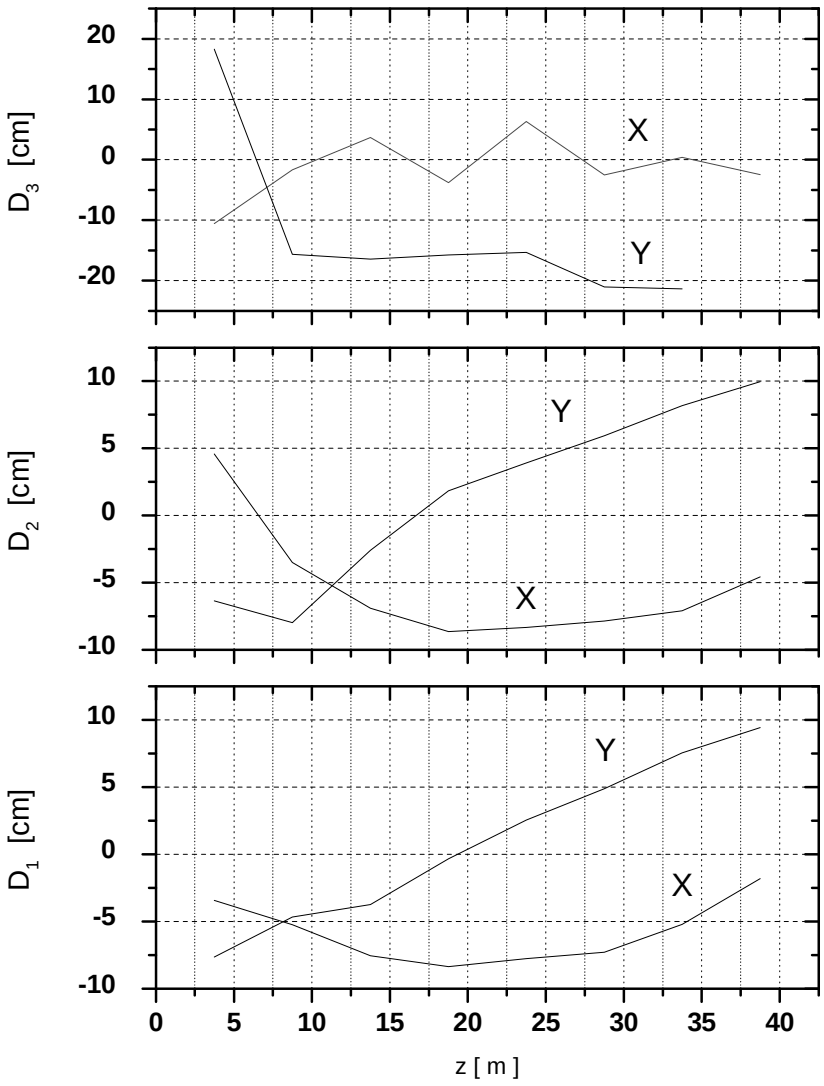

Figure 1 Dispersion as a function of z. D1 (bottom) has a solenoidal field of 6 T. D2 (middle) has a solenoidal field of 5 T. D3 (top) has a solenoidal field of 6 T and an initial beam correlation described in the text.

5 Reduction of energy spread

We now include wedge shaped absorbers in the simulation in order to reduce the energy spread. Once the wedges are included the mean energy of the beam drops and we must also taper the solenoid field strength to keep the Larmor period shorter than the fixed wiggler period. We use a linear solenoid field taper, varying from 6 T to 1.25 T over 40 m. The wedge geometry is shown in Fig. 2.

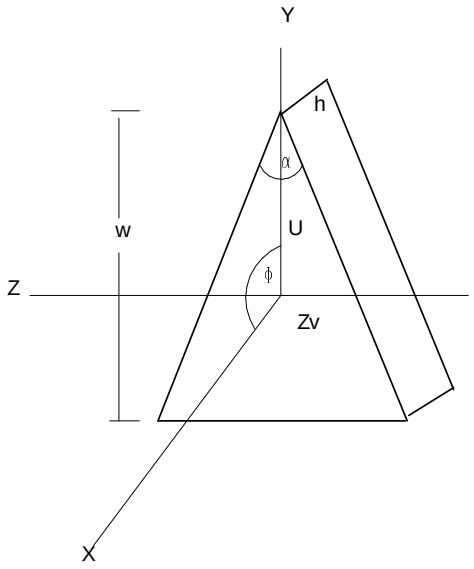

Figure 2 ICOOL wedge geometry.

The first 3.75 m at the beginning of the channel did not have wedges in order to allow the dispersion to build up. Following this wedges were located every half wiggler period. The wedge material was LiH, the opening angle α was 20^{o} and the overall dimensions of the wedges (*h, w*) were chosen to encompass over 99% of the beam.

We take an initial, on-axis muon beam with a gaussian distribution of momentum 500±50 MeV/c, 0 bunch length and 0 finite emittance. We first examine the cooling behavior with stochastic processes turned off. We used a fixed step size of 2 mm for the particle tracking.

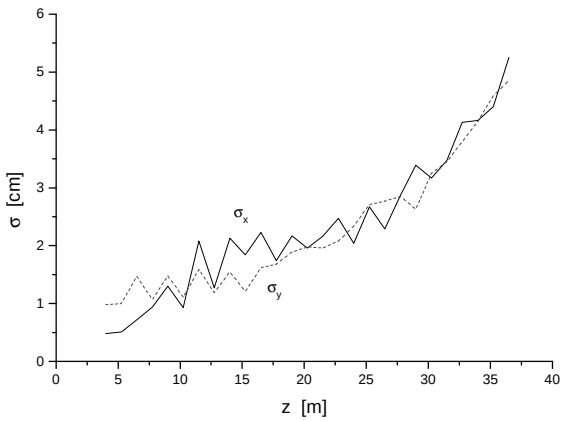

Figure 3 Transverse size of the beam as a function of distance down the channel.

The size of the beam, shown in Fig. 3, grows as it proceeds down the channel. This growth is due to a combination of the reducing solenoid strength and the dispersion.

We adjusted the azimuthal angle φ of each wedge in order to minimize the energy spread at that *z* location. The resulting azimuthal angle is shown in Fig. 4 as a function of *z* for two values of the dipole strength. We see that the optimum angle oscillates back and forth. The oscillations are large at the beginning of the channel, but then dampen out near the end. The optimized angles are similar for both dipole strengths.

The decrease in energy spread is shown in Fig. 5 for two values of the dipole strength. The system clearly does reduce the energy spread in the beam. Increasing the dipole strength leads to a smaller final energy spread in a shorter distance of channel. After reaching the minimum energy spread, further wedges cause the energy spread to begin increasing again. However, the magnitude of the reduction is small, e.g. ~28% over 28 m for the 0.3 T case in Fig. 5.

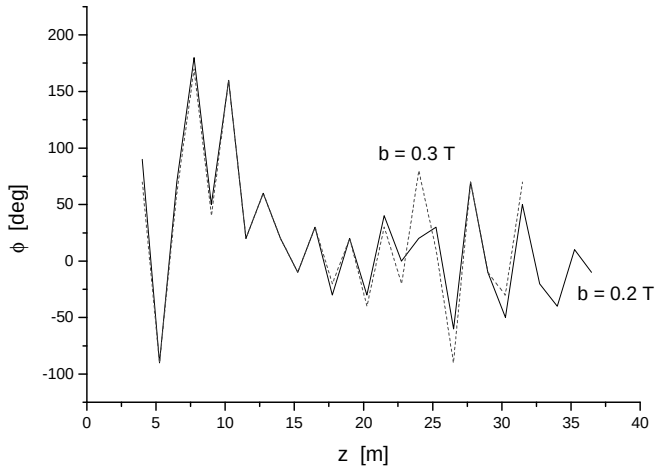

Figure 4 Optimized azimuthal angle φ of the wedges as a function of distance down the channel. Two values of the dipole strength *b* are shown.

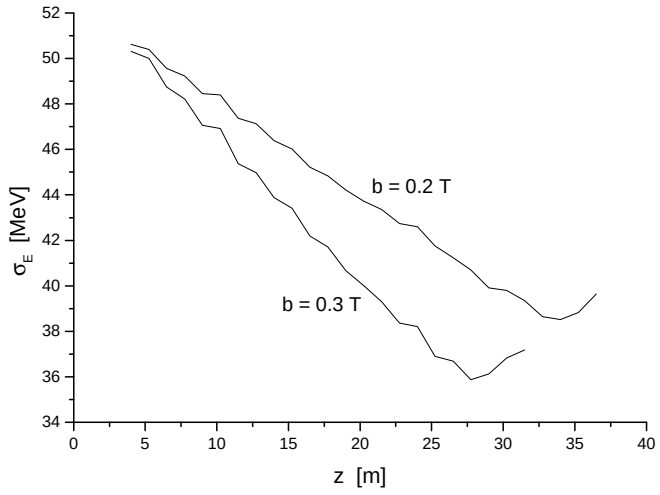

Figure 5 Energy spread of the beam as a function of distance down the channel. Two values of the dipole strength *b* are shown.

We show in Fig. 6 a comparison of the ideal case we have been considering with a case where we have included the effect of scattering and straggling in the wedges and where we include in addition the effect of finite transverse emittance in the beam.

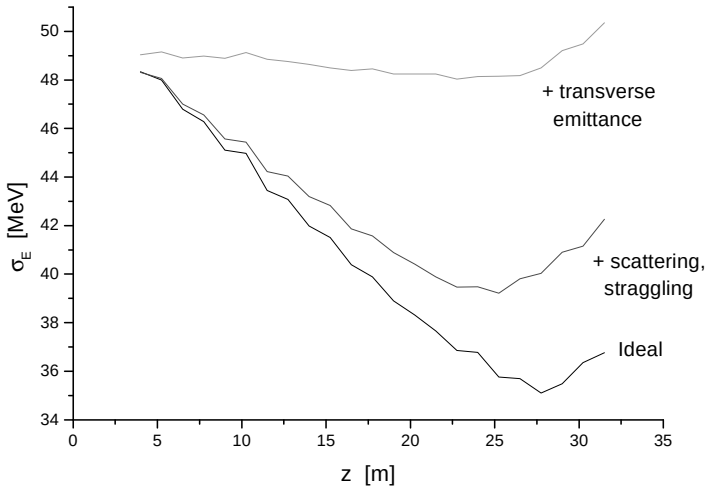

Figure 6 Energy spread as a function of distance down the channel.

Stochastic processes in the wedges significantly reduce the effectiveness of the cooling. The upper curve shows a case with $\sigma_X = \sigma_Y = 10$ mm and $\sigma_{Px} = \sigma_{Py} = 10$ MeV/c. Off-axis particles were given an initial angular momentum corresponding to the magnetic field strength. This corresponds to an initial normalized transverse emittance of 0.95 mm, much smaller than the 15 mm expected at the neutrino factory. The cooling effect was washed out for larger initial transverse emittances.

6 Conclusions

We have found that the helical sweeping method for reducing the energy spread works in principle. The rotating dipole field produces a dispersion ~10 cm for the parameters suggested in reference 3. Optimized azimuthally spaced wedges can remove energy spread from the beam. However, the amount of energy spread reduction is very small, ~30%, even for an ideal initial beam. The method does not appear to be practical for the huge emittance beam expected at the neutrino factory.

Acknowledgments

We would like to thank Yaroslav Derbenev for useful discussions.

Notes and references

[1] C. Ankenbrandt et al, Status of muon collider research and development and future plans, Phys. Rev. ST-AB 2:081001-1-73, 1999, p. 27-32.
[2] D. Neuffer, Phase space exchange in thick wedge absorbers for ionization cooling, in D. Cline (ed), Physics Potential and Development of $\mu^+\mu^-$ Colliders, AIP Conf. Proc. 441, 1998, p. 270-281.
[3] Y. Derbenev, Conceptual studies on ionization cooling of muon beam, NuMu note 185, 2000; Sweeping method to cool a large energy spread of initial muon beam, NuMu note 135, 2000; Resume on sweeping cooling and cooling agenda in general, NuMu note 133, 2000.
[4] T. Tominaka, Magnetic field calculation of helical dipole coils, AGS/RHIC Spin note 24, 1996.
[5] W. Kaplan, Advanced Calculus, Addison-Wesley, 1952, p. 63.
[6] H. Weidemann, Particle Accelerator Physics, Vol. 2, Springer, 1995, p. 51.